

Towards the Design of Linear Homo-Trinuclear Metal Complexes Based on a New Phenol-Functionalised Diazamesocyclic Ligand: Structural Analysis and Magnetism

Miao Du,^{*[a]} Xiao-Jun Zhao,^[a,b] Jian-Hua Guo,^[a] Xian-He Bu,^{*[b]} and Joan Ribas^{*[c]}

Keywords: Functionalised diazamesocyclic ligand / Copper(II) and Nickel(II) / Crystal structures / Magnetochemistry / Trinuclear complexes

The formation of two novel phenoxo-bridged linear trimetallic Cu^{II} and Ni^{II} complexes, [Cu₃(μ-L)₂](CH₃OH)₂(ClO₄)₂ (**1**) and [Ni₃(μ-L)₂](CH₃OH)₂(ClO₄)₂ (**2**), with a new diazamesocyclic ligand functionalised by additional phenol donor pendants (H₂L = *N,N'*-bis(2-hydroxybenzyl)-1,4-diazacycloheptane), has been achieved and both complexes have been characterised by IR spectroscopy, elemental analyses, conductivity measurements, thermal analyses and UV/Vis techniques. Single-crystal X-ray diffraction analyses revealed that both **1** and **2** have the similar phenoxo-bridged linear trinuclear cores. For **1**, two terminal and the central Cu^{II} ion are in square-planar environments with the adjacent intramolecular Cu...Cu separation of 2.9376(9) Å. For **2**, however, two terminal Ni^{II} ions are in square-planar environments and the central Ni^{II} ion assumes an octahedral geometry by axial coordination of two methanol ligands, the adjacent intramolecular Ni...Ni distance being 3.007(3) Å. In both cases, the 1,4-diazacycloheptane (DACH) ring adopts the normal boat

configuration. The magnetic properties of complexes **1** and **2** have been investigated by variable-temperature magnetic susceptibility measurements in the solid state. Complex **1** displays a very strong antiferromagnetic coupling interaction between the neighbouring μ-phenoxo Cu^{II} centres with a *J* parameter of -314 cm⁻¹ and the magneto-structural correlation for such complexes is discussed in detail. For complex **2**, the result indicates that both terminal Ni^{II} ions are diamagnetic and the central Ni^{II} shows typical paramagnetic behaviour. The presence of zero-field splitting for Ni^{II} with a *D* parameter of 11 cm⁻¹, being active at low temperature, is further corroborated by the magnetisation measurement at 2 K. Additionally, the interesting ESR spectra of **1** at different temperatures (from 298 K to 8 K) were investigated and interpreted.

(© Wiley-VCH Verlag GmbH & Co. KGaA, 69451 Weinheim, Germany, 2005)

Introduction

The development of routes and strategies for the design and preparation of polynuclear complexes of 3d metals in moderate oxidation states is of great importance in bioinorganic chemistry, magnetochemistry, materials chemistry and solid-state chemistry.^[1] Trinuclear compounds can be classified as linear or nonlinear according to the arrangements of the metal centres and a number of linear trinuclear compounds have been structurally and magnetically characterised to date.^[2] Of further importance is the fact that most of the known trinuclear complexes have two, three or four

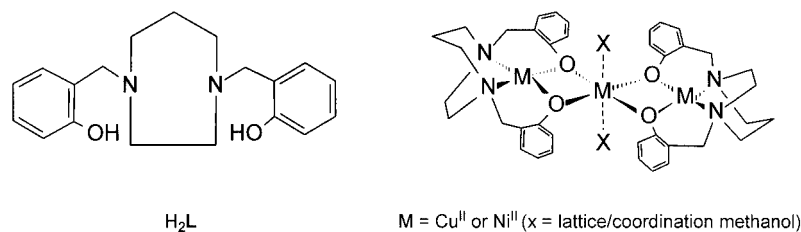
simple and/or intricate bridging ligands between the metal centres which usually contain simple anions such as chloride,^[3] hydroxide,^[4] acetate,^[5] methoxide^[6] or azide^[7] and only a minority of them have the M₃ core bridged by just a single organic ligand. Thus, the rational design and preparation of such trinuclear complexes still remains a difficult challenge and attracts continuing interest.

As described in many other publications by us, we have been exploring the coordination chemistry of diazamesocyclic systems, especially the typical 1,5-diazacyclooctane (DACO) which exhibits an exceptionally strong ligand field, a unique configuration and the potential for further functionalisation.^[8–11] It has been well demonstrated by us and others^[12] that DACO modified by suitable functional pendants, such as heterocyclic, phenolic, thiol and carboxylic groups could be used as good building blocks for constructing polymeric systems with unique structures and properties. Based on our experimental findings, a general rule for the coordination chemistry of functionalised DACO compounds has been established according to the types and numbers of the additional pendant arms. One of

[a] College of Chemistry and Life Science, Tianjin Normal University, Tianjin 300074, P. R. China
Fax: (internat.) +86-22-23540315
E-mail: dumiao@public.tpt.tj.cn

[b] Department of Chemistry, Nankai University, Tianjin 300071, P. R. China
E-mail: buxh@nankai.edu.cn

[c] Departament de Química Inorgànica, Universitat de Barcelona, Diagonal, 647, 08028 Barcelona, Spain
E-mail: joan.ribas@qi.ub.es



Scheme 1

the main reasons that justifies the continuous interest in such attractive system is the construction of other novel metal complexes with special frameworks and properties by modifying the backbone of the diazamesocycle, for example choosing 1,4-diazacycloheptane (DACH) as the initial material. Our preliminary results indicate that the metal complexes of the heterocycle-functionalised DACH derivatives usually exhibit similar structures to those of the corresponding DACO compounds but with a change in the coordination environments of the metal centres due to their different configurations (normally, boat-chair for DACO ring, and boat for DACH).^[13] It should be noted that almost all metal centres chelated to DACO derivatives assume pentacoordinate geometries^[8–12] but this is not the case for DACH.^[13] For metal complexes with the DACO ligand bearing two phenol arms, phenoxo-bridged linear trimetallic Cu^{II} and Ni^{II} frameworks were obtained. The former exhibits a square pyramid/square plane/square pyramid Cu₃ core^[10a] and the latter is the first square pyramid/octahedral/square pyramid Ni₃ complex.^[10b] Thus, as a continuation of our work, we report herein the design and preparation of a new phenol-functionalised DACH ligand *N,N'*-bis(2-hydroxybenzyl)-1,4-diazacycloheptane (H₂L, see Scheme 1) and its Cu^{II} and Ni^{II} complexes [Cu₃(μ-L)₂](CH₃OH)₂(ClO₄)₂ (**1**) and [Ni₃(μ-L)₂](CH₃OH)₂(ClO₄)₂ (**2**). The magnetic properties of both complexes have been investigated and the magneto-structural correlation between **1** and related compounds has been discussed. Of further interest is the fact that relatively few trinuclear Cu^{II} compounds have been studied by ESR techniques^[14] and, thus, the ESR properties of **1** at different temperatures (from 298 K to 8 K) were analysed in detail in this study.

Results and Discussion

Preparation, Characterisation and Spectra of Compounds **1** and **2**

The new ligand H₂L was synthesised using an excess of 2-bromomethyl phenylacetate in order to largely obtain the doubly substituted product as described in detail in our previous report.^[10a] The yield was moderate. All analytical and spectroscopic data are in good agreement with the theoretical requirements. The preparations of **1** and **2** were achieved directly by treatment of the ligand with the corresponding metal perchlorate and the ligand becomes doubly deprotonated when forming the metal complex.

In the IR spectra of H₂L and both complexes, the absorption bands resulting from the skeletal vibrations of the aromatic rings appear in the 1400–1600 cm⁻¹ region. The broad band centred at ca. 3400 cm⁻¹ results from the O–H stretching of the phenol groups (for H₂L) or the solvent methanol molecules (for **1** and **2**). The very strong bands at 1256 cm⁻¹ (for H₂L), 1264 and 1247 cm⁻¹ (for **1**) and 1261 cm⁻¹ (for **2**) are the characteristic absorptions of the C–O groups of the phenol pendant arms. Additionally, in the IR spectra of both complexes, the strong bands that appear at ca. 1100 and 624 cm⁻¹ suggest the presence of the perchlorate anions.^[15]

The UV/Vis spectra of complexes **1** and **2** (CH₃CN and H₂O, respectively) have been investigated at room temperature. It is important to know the structures of the complexes in solution prior to spectroscopic discussions. Thus, the conductivities of both complexes were measured and the molar conductivities of **1** and **2** indicate both complexes behave as the typical 2:1 electrolytes in the corresponding solution, this being consistent with their solid structures. Evidently the phenoxo bridges are retained in solution. The visible spectrum of **1** shows a moderate shoulder band at ca. 558 nm and a more intense absorption band at 386 nm which can be assigned to the *d–d* component of Cu^{II} ions with a square-planar geometry and the charge-transfer (CT) transition band from the filled *p*_π orbital of the phenolic oxygen to the vacant *d* orbitals of Cu^{II}, respectively.^[16] For complex **2**, two such types of absorptions appear at 498 nm and 362/324 nm (one is due to the terminal Ni^{II} CT and the other to the central Ni^{II} CT with different coordination geometries^[2c]), respectively. In addition, the intense bands observed in the 200–300 nm region in the spectra of both complexes can be attributed to the π→π* ligand transitions.

Both **1** and **2** are air stable at room temperature but decomposition occurs at elevated temperature, however. Thermogravimetric analyses (from room temperature to 600 °C) indicate that for **1**, the first weight loss of 6.44% from 118 to 164 °C (peak: 132 °C) corresponds to the loss of two CH₃OH solvent molecules (calculated: 5.96%). The remaining substance does not lose weight upon further heating until a rapid weight loss in the 244–264 °C region (peak: 258 °C). Further heating to 600 °C induces a continuous and slow weight loss. The thermal behaviour of **2** is similar to **1**, the first weight loss of 5.84% from 85 to 160 °C (peak: 138 °C) corresponds to the release of two coordinated methanol ligands (calculated: 6.04%). The remaining coord-

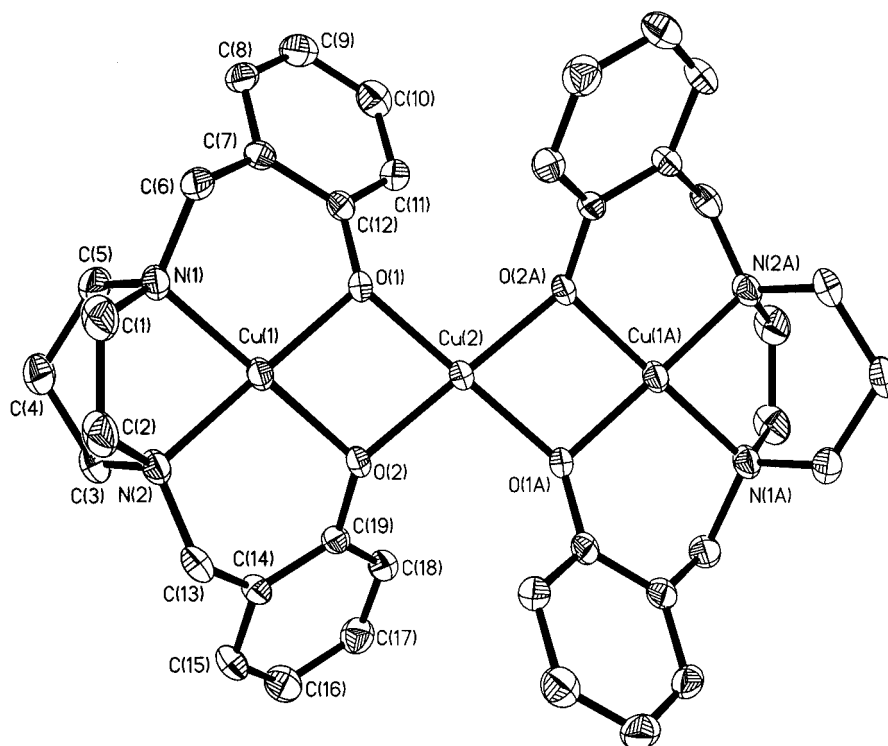


Figure 1. ORTEP view of the molecular structure of **1** including atomic labelling of the asymmetric unit (hydrogen atoms, perchlorate anions and methanol solvents are omitted for clarity) with displacement ellipsoids drawn at the 30% probability level

minated framework does not lose weight upon further heating until two consecutive weight losses occur in the 270–325 °C region (peak: 288 and 312 °C). As for **1**, further heating to 600 °C only shows a continuous and slow weight loss.

Single-Crystal X-ray Structures of Complexes **1** and **2**

Structure Description of $[\text{Cu}_3(\mu\text{-L})_2](\text{CH}_3\text{OH})_2(\text{ClO}_4)_2$ (**1**)

An ORTEP diagram of complex **1** is shown in Figure 1 and selected bond lengths and angles are listed in Table 1. The structure consists of a discrete $[\text{Cu}_3(\mu\text{-L})_2]^{2+}$ cation in which the ligands are doubly deprotonated, two perchlorate counter anions and two lattice methanol solvent molecules. The asymmetric unit is formed by half a molecule which exhibits inversion in the centre of the rhombohedron which itself consists of four phenol oxygen atoms [Cu(2) is just on this inversion centre]. Two terminal Cu(1) and Cu(1A) atoms, located in general positions, are centrosymmetrically related to each other and, hence, three Cu^{II} ions linked by the phenoxo bridges lie in a straight line. Each terminal Cu^{II} ion is coordinated to two nitrogen atoms from the DACH ring (Cu–N distances: 1.973(3) and 1.981(3) Å) and two phenolate oxygen donors (Cu–O lengths: 1.927(3) and 1.928(3) Å), adopting an approximately square-planar geometry (CuN_2O_2). The central Cu(2) atom is coordinated to four bridging phenolate oxygens (Cu–O lengths:

1.956(3) and 1.953(3) Å) which further link the other two Cu^{II} ions to form the linear Cu_3 array, resulting in a CuO_4 plane. Additionally, weak interactions between the central Cu(2) and the perchlorate anions (located in the axial position of the Cu^{II} coordination sphere) can be observed with a Cu(2)–O(3) distance of 2.589(3) Å which is significantly longer than the normal Cu–O coordination bond. The terminal Cu(1) ion is only ca. 0.035 Å above the basal least-squares plane and the central Cu(2) is located exactly on its coordination plane due to the site symmetry. The folding angle between the perfect square plane O(1)–O(1A)–O(2)–O(2A) and the best calculated plane N(1)–N(2)–O(1)–O(2) is 10.8° and the dihedral angle between the two Cu(1)–O(1)–Cu(2) and Cu(1)–O(2)–Cu(2) planes is 10.9°. The intramolecular Cu...Cu separation is 2.9376(9) Å whereas the Cu(1)–O–Cu(2) bridging angles are 98.31(12) and 98.38(11)° for O(1) and O(2), respectively. For the ligand, the DACH ring takes the normal boat configuration and the dihedral angle between two phenol planes is 117.6°. A pair of nitrogen atoms from DACH and two oxygen atoms of phenolate pendant arms are in *cis* positions in the coordination plane of the chelated Cu(1) atom.

Analysis of the crystal packing of complex **1** indicates that the trimers are well isolated in the unit cell, with the intermolecular contacts between the Cu^{II} centres above 5.8 Å. There exists only an intramolecular O(7)–H(7)···O(3) hydrogen bond between the methanol molecule and the per-

Table 1. Selective bond lengths (Å) and angles (°) for complex **1**

Bond lengths			
Cu(1)–O(1)	1.927(3)	Cu(1)–O(2)	1.928(3)
Cu(1)–N(1)	1.973(3)	Cu(1)–N(2)	1.981(3)
Cu(2)–O(1)	1.956(3)	Cu(2)–O(2)	1.953(3)
C(12)–O(1)	1.364(5)	C(19)–O(2)	1.379(4)
Cu(1)–Cu(2)	2.9376(9)		
Bond angles			
O(1)–Cu(1)–O(2)	81.89(11)	O(1)–Cu(1)–N(1)	98.73(13)
O(2)–Cu(1)–N(1)	178.79(13)	O(1)–Cu(1)–N(2)	176.92(13)
O(2)–Cu(1)–N(2)	97.83(13)	N(1)–Cu(1)–N(2)	81.49(14)
O(2)–Cu(2)–O(1)	80.52(11)	O(2)–Cu(2)–O(1) ⁱ	99.48(11)
Cu(1)–O(1)–Cu(2)	98.31(12)	Cu(1)–O(2)–Cu(2)	98.38(11)
Symmetry code: (i) 1 – x, 1 – y, 1 – z			

chlorate anion. The O···O separation is 2.995 Å with an H···O distance of 2.242 Å and the bond angle is 152.7° which is in the normal range for such a weak interaction.^[17]

Structure Description of [Ni₃(μ-L)₂(CH₃OH)₂](ClO₄)₂ (**2**)

A single-crystal X-ray determination indicates that the structure of complex **2** consists of a [Ni₃(μ-L)₂(CH₃OH)₂]²⁺ cation exhibiting a similar M₃ framework to **1** and two perchlorate anions. Selected bond lengths and angles for **2** are listed in Table 2. As depicted in Figure 2, the asymmetric unit is formed by half of the complex which shows an inversion centre [Ni(2)] in the middle of the rhombohedral plane. Since Ni(2) occupies the inversion centre, the resultant Ni(1)–Ni(2)–Ni(1A) array is linear. As in **1**, a pair of nitrogen atoms from DACH (Ni–N distances: 1.903(4) and 1.897(4) Å) and two oxygen atoms of the phenolate pendant arms (Ni–O lengths: 1.872(3) and 1.873(3) Å) are in a *cis* position. These positions constitute the approximate coordi-

Table 2. Selective bond lengths (Å) and angles (°) for complex **2**

Bond lengths			
Ni(1)–O(1)	1.872(3)	Ni(1)–O(2)	1.873(3)
Ni(1)–N(1)	1.903(4)	Ni(1)–N(2)	1.897(4)
Ni(2)–O(1)	2.040(3)	Ni(2)–O(2)	2.050(3)
Ni(2)–O(3)	2.067(3)	Ni(1)–Ni(2)	3.007(2)
C(12)–O(1)	1.357(5)	C(19)–O(2)	1.361(5)
Bond angles			
O(1)–Ni(1)–O(2)	83.75(12)	O(1)–Ni(1)–N(1)	96.61(14)
O(2)–Ni(1)–N(1)	178.27(15)	O(1)–Ni(1)–N(2)	178.93(15)
O(2)–Ni(1)–N(2)	96.48(14)	N(1)–Ni(1)–N(2)	83.12(16)
O(2)–Ni(2)–O(1)	75.33(11)	O(2)–Ni(2)–O(1) ^j	104.67(11)
O(3)–Ni(2)–O(1)	87.43(11)	O(3)–Ni(2)–O(1) ^j	92.57(11)
O(3)–Ni(2)–O(2)	88.29(12)	O(3)–Ni(2)–O(2) ^j	91.71(13)
Ni(1)–O(1)–Ni(2)	100.39(13)	Ni(1)–O(2)–Ni(2)	98.98(14)
Symmetry code: (i) 1 – x, –y, 1 – z			

dination plane of the terminal Ni(1) atom with a derivation from planarity of 0.022 Å. However, the central Ni(2) is six-coordinate: four phenol oxygen atoms are in the equatorial plane with Ni–O distances of 2.040(3) and 2.050(3) Å with two methanol ligands occupying the axial positions with Ni–O lengths of 2.067(3) Å. Thus, the coordination environment of Ni(2) can be described as a slightly distorted elongated octahedron with the *cis* O–Ni–O angles being in the range of 75.33(11)–104.67(11)°. In **2**, the folding angle between the perfect square plane O(1)–O(1A)–O(2)–O(2A) and the best calculated plane N(1)–N(2)–O(1)–O(2) is 6.3° and the dihedral angle between the two Ni(1)–O(1)–Ni(2) and Ni(1)–O(2)–Ni(2) planes is 8.7°. The intramolecular Ni···Ni separation is 3.007(2) Å and the Ni(1)–O–Ni(2) bridging angles are 100.39(13) and 98.98(14)° for O(1) and O(2), respectively. For the doubly deprotonated ligand, the DACH ring assumes the normal boat configuration and the dihedral angle between two phenol planes is 56°. Similar to **1**, the trinuclear subunits are well isolated in the unit cell with the intermolecular contacts between the Ni^{II} centres above 6.0 Å. An intramolecular O(3)–H(3C)···O(4) hydrogen-bonding interaction between the coordinated methanol molecule and the perchlorate anion can be observed and this further stabilises the structure. The O···O separation is 2.861 Å with an H···O distance of 2.074 Å and the bond angle is 160.8°, which is in the normal range for such weak interactions.^[17]

ESR Spectra of Complex **1**

For the interpretation of the ESR spectra of complex **1**, it is convenient to consider the relative energies of the states deduced by coupling the three *S* = 1/2 ions. A demonstration of these states and the corresponding energies can be found in the book of O. Kahn.^[18] The spin diagram is given in Figure 3 in which the occurrence of *ZFS* in the state |3/2, 1/2> is considered, giving two doublets corresponding to *m_s* = ± 3/2 and ± 1/2. As shown, *m_s* = ± 1/2 is strongly anisotropic.^[19]

The ESR spectra of **1**, as a function of temperature, are given in Figure 4. The easiest spectrum to interpret is that corresponding to the lowest temperature measured (8 K). The spectrum shows a very narrow almost isotropic band centred at *g* = 2.05. When the temperature is raised this signal broadens and at close to liquid nitrogen temperature it begins to appear as broad band near 1500 Gauss. The intensity of the spectrum diminishes as the temperature increases and at 298 K (final temperature we measured) the spectrum shows two clear and very broad signals, the first one centred at 3000 G (*g* = 2.08) and a new band centred at 1200–1300 G which corresponds to a *g* value of approximately 5.15. It must be pointed out that the difference in the intensities of the limiting spectra (room temperature and 8 K) is in the region of five orders of magnitudes (10⁵).

At low temperature, only the |1/2, 1> ground state is populated (*J* = –314 cm^{–1} according to the susceptibility measurements as described below). Thus the strong signal

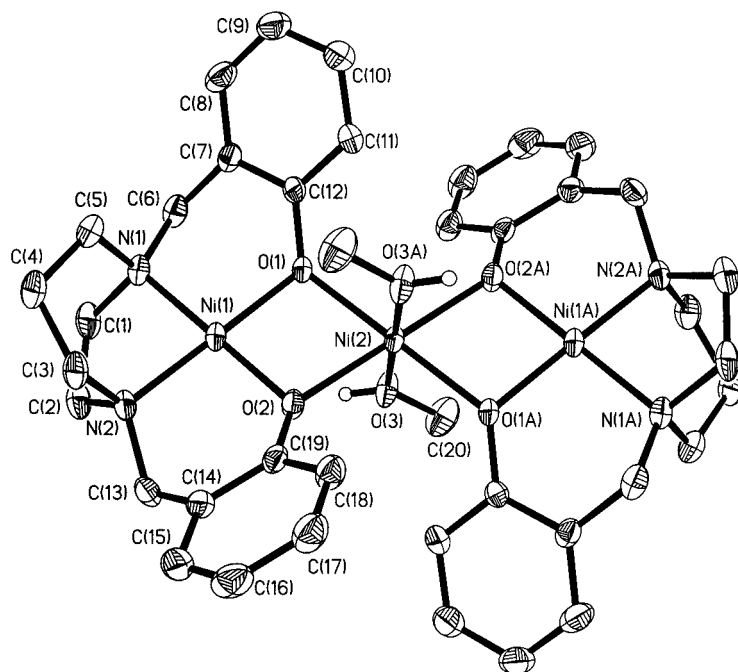


Figure 2. ORTEP structure of the molecular structure of **2** including atomic labelling of the asymmetric unit (hydrogen atoms and perchlorate anions are omitted for clarity) with displacement ellipsoids drawn at the 30% probability level

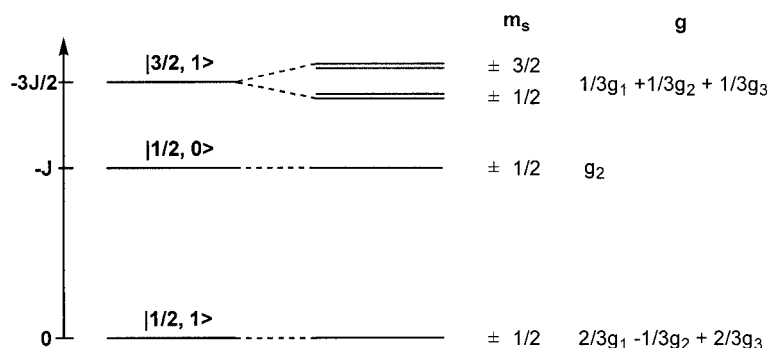


Figure 3. Spin levels, energies and g values in a trinuclear Cu_3 complex ($J < 0$)

at $g = 2.05$ is due to this ground state. This g value is an average of the g values of the three Cu^{II} ions ($g = 1/3 [2g_{\text{T1}} - g_{\text{C}} + 2g_{\text{T2}}]$ where C and T are the central and terminal Cu ions).^[19,20] The g values for the $|1/2, 0\rangle$ and $|3/2, 1\rangle$ states are different, provided that the individual g_i values are different.^[20] If we assume that the rate of transition from the lowest to the excited multiplets is fast on the ESR time scale, the observed spectrum at a given temperature would be the thermal average of the spectra of three different multiplets. Therefore, the liquid helium temperature spectra should be those of the lowest doublet, while those at higher temperatures should also bear the contributions of the excited multiplets. For this reason, the anisotropy of the molecular g value is usually not well defined. Only in a few trinuclear Cu^{II} complexes is this anisotropy manifested.^[21] In complex **1**, the observed g value is an average of two different Cu^{II} environments. On the other hand, in

solid state, the trinuclear cations are not perfectly isolated from a magnetic point of view. Effectively, we have found a nonnegligible J' value (molecular-field approach, see below). As has been pointed out,^[22] even an extremely weak value for the intermolecular exchange interaction leads to the exchange averaging effect which is responsible for the isotropic or quasi-isotropic spectra observed (such as in complex **1**).

Only on a few occasions for this kind of trinuclear Cu^{II} complex, has any evidence of signals attributable to a spin quadruplet been found. In contrast, this spin quadruplet is clearly visible at 4 K when the coupling is ferromagnetic because this is the ground state in this case.^[5,23] A broad transition between $g = 4.25-5.5$ occurs and can be assigned to the transition between the $\pm 1/2$ levels of the $S = 3/2$ system. Thus, this is undoubtedly the origin of the broad signal centred at $g \approx 5$ in complex **1**.

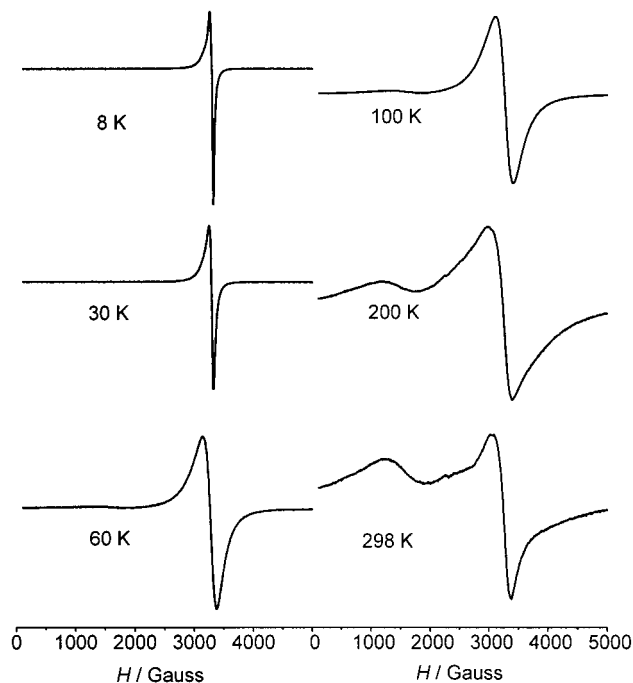


Figure 4. X-band powder ESR spectra at different temperatures for complex **1**; the ratio of the intensities at 8 K and 298 K is 10^5

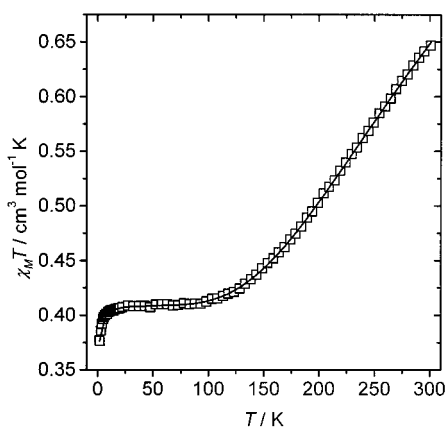


Figure 5. Plot of the temperature dependence of $\chi_M T$ for **1**; the solid line corresponds to the best fit (see text for parameters calculated)

Magnetic Properties of **1** and **2**

Complex **1**

The magnetic properties of complex **1** in the form of a $\chi_M T$ vs. T plot are shown in Figure 5 (magnetic susceptibility per three Cu^{II} ions). The $\chi_M T$ value is $0.65 \text{ cm}^3 \text{ mol}^{-1} \text{ K}$ at 300 K which is far from the value of $1.2 \text{ cm}^3 \text{ mol}^{-1} \text{ K}$ corresponding to three isolated spin doublets. The $\chi_M T$ value decreases to $0.40 \text{ cm}^3 \text{ mol}^{-1} \text{ K}$ upon cooling to ca. 80 K. At this point there is a clear plateau from 80 K to 10 K and, finally, there is a slight decrease to $0.38 \text{ cm}^3 \text{ mol}^{-1} \text{ K}$ at 2 K. This curve suggests strong antiferromagnetic coupling between the Cu^{II} centres with the presence of very small intermolecular antiferromagnetic interactions

being active only at very low temperature. Thus, in the light of the above structural discussion of complex **1**, we can interpret its magnetic behaviour through a simple model with only one intramolecular J parameter using the following spin Hamiltonian:

$$H = -J_1 (S_1 S_2 + S_2 S_3)$$

From this Hamiltonian it is possible to deduce a simple equation for $\chi_M T$ vs. T :^[18]

$$\chi_M T = \frac{Ng^2\beta^2[1 + \exp(J/KT) + 10\exp(3J/2KT)]}{4K[1 + \exp(J/KT) + 2\exp(3J/2KT)]}$$

This equation has been completed by introducing a J' parameter and considering the possible small interactions between the trinuclear entities using the molecular-field approach:^[18]

$$\chi_M = Ng^2\beta^2 F(J, T) / (kT - zJ'F(J, T))$$

The fit of the magnetic data, assuming that the g factors are identical for $\text{Cu}(1)$ and $\text{Cu}(2)$, leads to $J = -314.0 \pm 0.8 \text{ cm}^{-1}$, $J' = -0.5 \pm 0.01 \text{ cm}^{-1}$, $g = 2.09$ and $R = 1.5 \times 10^{-6}$ (R is the agreement factor defined as $\sum_i [(\chi_M T)_{\text{obs}} - (\chi_M T)_{\text{calc}}]^2 / \sum_i [(\chi_M T)_{\text{obs}}]^2$).

Magneto-Structural Correlations in Cu_2O_2 Cores

Magneto-structural correlations in dinuclear Cu^{II} complexes bridged equatorially by pairs of hydroxo^[24] or alkoxo^[25] groups show that the major factor controlling the spin coupling between the $S = 1/2$ metal centres is the $\text{Cu}-\text{O}(\text{R})-\text{Cu}$ angle. Hatfield and Hodgson found a linear correlation between the experimentally determined exchange coupling constant and the $\text{Cu}-\text{O}-\text{Cu}$ bond angle (ϕ) (see a in Figure 6).^[24] Antiferromagnetic behaviour is observed for complexes with ϕ larger than 97.6° , while ferromagnetism appears for those with smaller values of ϕ . An apparently similar linear relationship for the alkoxo cases^[25] shows that at angles around 95.6° , the exchange integral approaches zero, i.e. the point of experimental "accidental orthogonality". For such dimeric Cu^{II} complexes, Nieminen^[26] described correlations between the singlet-triplet splitting energy and the $\text{Cu}-\text{O}-\text{Cu}$ angle ϕ , the deviation d_c of the carbon atom connected to the bridging oxygen atoms from the $\text{Cu}-\text{O}-\text{Cu}$ plane and the sum of the angles around the bridging oxygen atoms. Walz et al.^[27] reported the influence of the coordination geometry around the Cu^{II} atom on the exchange interaction in alkoxo-bridged complexes. These experimental observations are consistent with studies using the angular overlap approach by Bencini and Gatteschi^[28] as well as extended Hückel MO treatments by Hoffmann^[29] and Kahn.^[30] More recent ab initio and DFT calculations on simple model dimers examined the effects of the bridging angles, $\text{Cu}-\text{O}$ distances, fold (hinge) angle along the $\text{O}-\text{O}$ axis and degree of tetrahedral (for square-planar geometry) or $sp \rightarrow bpt$ (for square-pyramidal geometry) distortions at the Cu^{II} centres.^[25,31–33] These theoretical studies showed that although the major factor affecting the magnetic exchange is the $\text{Cu}-\text{O}-\text{Cu}$

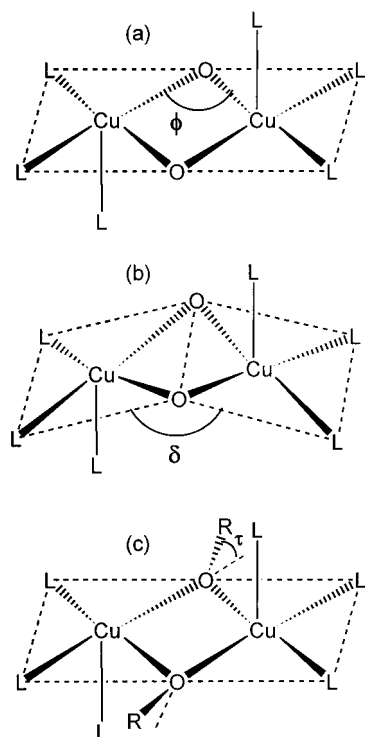


Figure 6. The three main factors in the Cu_2O_2 entities that tune the antiferromagnetic coupling in μ -phenoxo derivatives

bridge, other features can also significantly lead to the increase in the ferromagnetic contributions which effectively reduces any antiferromagnetic term associated with the hydroxo/alkoxo bridges. Among these features, we can underline the distortions of the coordination geometry of the Cu^{II} centre,^[34,35] the variation in $\text{Cu}-\text{O}$ bond lengths,^[32] the hinge (roof shape) distortion of the core (δ , see b in Figure 6),^[31–33,36] the torsion angle created by the H (or R) group with regard to the Cu_2O_2 plane (τ angle, see c in Figure 6)^[32] and different electronic factors.^[31,32,37,38] Some of these geometric factors are shown in Figure 6.

Roughly the same features discussed for the hydroxo-bridged complexes also seem apparent in alkoxo-bridged complexes. Thompson et al. found significant differences in magnetic coupling between μ -hydroxo (or μ -alkoxo) and μ -phenoxo complexes.^[39] From this work, it is apparent that the slopes of the graphs ($2J$ vs. $\text{Cu}-\text{O}-\text{Cu}$ angle) of the hydroxo and alkoxo cases are comparable but the absolute values of $-2J$ are larger for the alkoxo species. However, the slope of the graph for the phenoxo system is smaller and the absolute values of $-2J$ are inherently larger. For lower angles (95°) the J values approach zero for the alkoxo species but this is not the case for phenoxo bridging complexes. The range of the average angles for these phenoxo complexes is very small (from 99 to 105°). The couplings lie between -700 cm^{-1} (for smaller angles) and -900 cm^{-1} (for larger angles) as shown in Figure 7.^[39] For $J = 0$ the $\text{Cu}-\text{O}-\text{Cu}$ angle should be 77° , although this angle has not been experimentally observed at present. The observation of greater J values for $-\text{OR}$ than $-\text{OH}$ is due to the

effect of replacing the hydrogen of the hydroxo with a more electronegative carbon group which reduces the electron density on the oxygen bridge.^[36]

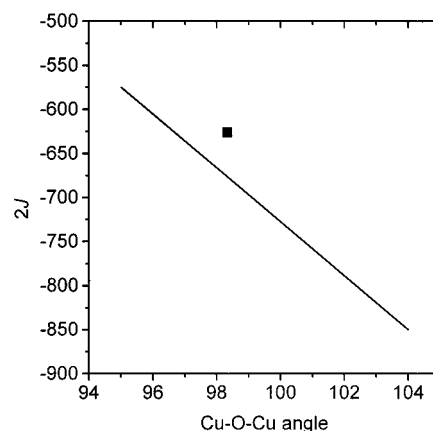


Figure 7. Schematic plot of the $2J$ values vs. $\text{Cu}-\text{O}-\text{Cu}$ angles given by Thompson et al. in ref.^[42] together with the point indicating the experimental value for **1**; in this figure the symbolism of $2J$ has been kept, although in the text we have used the Hamiltonian $-J$ instead of $-2J$.

Similar correlations can be established for comparable macrocyclic dicopper(II) systems, such as “Robson” type macrocyclic complexes, formed by Cu^{II} ions acting as templates for the condensation of diformylphenols and various diamines. These systems contain phenoxo oxygen atoms bridging the two Cu^{II} centres and represent ideal systems for examining the exchange coupling via the phenoxo oxygen. The degree of distortional flexibility available to simple dimeric Cu^{II} complexes with hydroxo or alkoxo bridges can be expected to be reduced when the $\text{Cu}-(\text{O})_2-\text{Cu}$ entity is enclosed within the cavity of a macrocyclic ligand and, thus, one might expect a more straightforward relationship between the bridging angle and the exchange with respect to electronic perturbations. Only a few structural examples of this sort of complex have been reported in which the linker group between the azomethanide nitrogens is two-membered, thereby creating a five-membered chelate ring.^[39] The $\text{Cu}-\text{O}_{\text{phenoxo}}-\text{Cu}$ angles fall in the range $98.8-100.9^\circ$, this being at the lower end of the range of angles typical for phenoxo systems. In all cases, the molecules themselves and the dinuclear centres are almost flat. There are no unusual structural or electronic perturbations which might be expected to influence the exchange in a significant way in those complexes. Thus, the phenoxo bridging angle can be considered to be the principal factor controlling the spin coupling.

In summary, the main conclusion for phenoxo systems is that strong antiferromagnetic exchange will dominate in these complexes. For comparison with complex **1**, structural and magnetic parameters for some related $[\text{Cu}_2(\mu\text{-OR})]$ complexes are listed in Table 3. In the present case, complex **1** belongs to the μ -phenoxo-bridged group of complexes. The $\text{Cu}-\text{O}-\text{Cu}$ angles are $98.31(12)$ and $98.38(11)^\circ$, respectively, and the intramolecular $\text{Cu}\cdots\text{Cu}$ separation is $2.9376(9)\text{ \AA}$. The hinge angle (δ) through the $\text{O}(1)-\text{O}(2)$

Table 3. Structural and magnetic parameters for some relevant [Cu₂(μ-OR)₂] complexes (basal-basal coordination)

Compound	φ ^[a]	τ ^[a]	δ ^[a]	<i>J</i>	Ref.
[Cu(L)(CH ₃ COO) ₂](<i>O</i> -acetato)	95.7/102.6	–	–	≈ +1	[40]
[Cu(AE)(CH ₃ COO) ₂](<i>O</i> -acetato)	95.34	–	180	≈ –1	[41]
[Cu(bpy) ₂ {μ-Ph(OCH ₂)Npy} ₂]- (ClO ₄) ₂ (alkoxo)	97.8	62	180	+10 (2 <i>J</i>)	[42]
[Cu(phen) ₂ {μ-Ph(OCH ₂)Npy} ₂]- (ClO ₄) ₂ (alkoxo)	98.3	48.7	180	–98 (2 <i>J</i>)	[42]
[Cu ₂ (b2b) ₂ (OR) ₂](ClO ₄) ₂ (alkoxo)	130.21	–	180	diamag.	[43]
[Cu ₂ (b3b) ₂ (OR') ₂](ClO ₄) ₂ (alkoxo)	102.9	–	180	diamag.	[43]
[Cu(papen)] ₂ ·2H ₂ O (alkoxo)	98.3	–	164.1	–128 (2 <i>J</i>)	[48]
[Cu ₂ (HL) ₂](NO ₃) ₂ (phenoxo no-macro)	102.8/103.1	–	141.1	–714	[44]
[Cu ₂ (L)(HL)](ClO ₄) (phenoxo no-macro)	103.81/101.8	–	–	–277	[44]
[Cu ₂ (fsa ₂ en)] (phenoxo no-macro)	100.1	–	–	–650 (2 <i>J</i>)	[45]
[Cu(etsal)NO ₃] ₂ (phenoxo no-macro)	101.1	–	180	–166 (2 <i>J</i>)	[46]
[Cu(ips)Cl] ₂ (phenoxo no-macro)	103.6	–	180	–145	[34]
[Cu ₂ (L1)(H ₂ O) ₂]F ₂ (phenoxo macro)	103.65	–	180	–790	[39]
[Cu ₂ (L2)Cl ₂][Cu ₂ (L2)(H ₂ O) ₂]Cl·ClO ₄ (phenoxo macro)	105 (av)	–	–	–800	[39]
[Cu ₂ (L3)(H ₂ O) ₂]BF ₄ (phenoxo macro)	98.8	–	180	–690	[39]
[Cu ₂ L1(ClO ₄) ₂] (phenoxo macro)	102.8	–	180	–740	[47]

^[a] The meaning of Greek symbols is given in Figure 6.

axis is 170°, i.e. very close to 180° which corresponds to an exactly planar structure. The torsion angles (τ) created by C(19) and C(12) (phenoxo ligands) from the Cu₂O₂ plane are 140/147.2 and 138.9/145.6°, respectively. Thus, we can expect strong antiferromagnetic coupling as experimentally observed. Plotting the 2*J* values indicated by Thompson et al. in reference 42 and adding the Cu–O–Cu angles and the 2*J* parameter for complex **1**, a rather good agreement can be observed (Figure 7). The difference could be due to the hinge angle (very small in this case) and, mainly, to the τ distortion (considerable in complex **1** as stated above).

Complex 2

The magnetic properties of **2** in the form of χ_M*T* vs. *T* plots are shown in Figure 8, these representing the magnetic

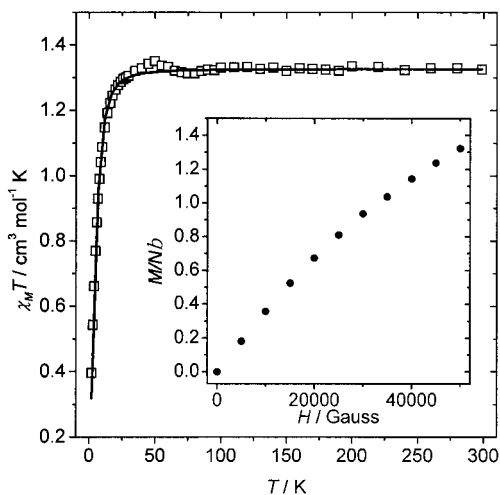


Figure 8. Plot of χ_M*T* vs. *T* for complex **2**; the solid line in the χ_M*T* curve represents the best fit for calculating the *D* value (see text); inset: plot of the reduced magnetisation (*M/Nβ*) vs. *H* at 2 K for complex **2**

susceptibility *per* Ni^{II} ion (the terminal ones are diamagnetic). The χ_M*T* value is 1.32 cm³ mol^{–1} K at 300 K which is a typical value for an isolated Ni^{II} ion with *g* > 2.00. χ_M*T* is practically constant to 25 K and then decreases to 0.3 cm³ mol^{–1} K at 2 K. This feature suggests typical paramagnetic behaviour for a Ni^{II} ion in which the *D* parameter and/or intermolecular interactions (usually antiferromagnetic) are active at low temperature. In an attempt to calculate the *D* value, we have fitted the experimental χ_M*T* values to the formula given by Kahn for a mononuclear Ni^{II} ion taking into consideration the *ZFS* of the *S* = 1 ground state.^[18] The best fit values are |*D*| = 11 cm^{–1} and *g* (average) = 2.30. The *D* value is higher than that typical for Ni^{II} ions (close to 5–8 cm^{–1}), indicating that the possible intermolecular interactions are superimposed on this *D* value. The magnetisation measurement at 2 K corroborates the effect of the *D* parameter, i.e. the reduced magnetisation (*M/Nβ*) at 5 T is only consistent with 1.4 electrons instead of two electrons which should be the theoretical value for an isolated Ni^{II} ion with *g* = 2.00 (see inset in Figure 8).

Conclusions and Perspectives

Two novel linear phenoxo-bridged trinuclear Cu^{II} and Ni^{II} complexes were rationally designed and prepared based on a new diazamesocyclic ligand bearing two pendant phenol donors. From a magnetic point of view, the data for complex **1** show two features: the very strong antiferromagnetic coupling interaction between the neighbouring μ-phenoxo Cu^{II} centres and the small possible interactions between the trinuclear entities. The magneto-structural correlations for related complexes containing Cu₂O₂ cores have been analysed in detail. For **2**, both terminal Ni^{II} ions are diamagnetic and the central Ni^{II} shows typical paramagnetic behaviour. The zero-field splitting for Ni^{II} can be ob-

served and further corroborated by the magnetisation measurements. Additionally, the interesting ESR properties of **1** at different temperatures (from 298 K to 8 K) were investigated. Further studies of the coordination chemistry of such attractive systems are under way in our laboratory.

Experimental Section

Materials and Physical Measurements: With the exception of 2-bromomethyl phenylacetate, which was synthesised according to the reported literature procedure,^[49] all of the starting materials and solvents for the syntheses and the analyses were obtained commercially and used as received. ¹H NMR spectra were recorded on a Bruker AC-P 400 spectrometer (400 MHz) at 25 °C with tetramethylsilane as the internal reference. FT-IR spectra (KBr pellets) were recorded on an AVATAR-370 (Nicolet) spectrometer and electronic spectra were acquired with a CARY300 (Varian) spectrophotometer. C, H and N analyses were performed on a CE-440 (Leemanlabs) analyser. Conductivities of the complexes were measured at room temperature using a DDS 11A conductometer. Thermal stability (TGA) experiments were carried out on a Dupont thermal analyser from room temperature to 600 °C under a nitrogen atmosphere at a heating rate of 10 °C/min.

Synthesis of the Ligand *N,N'*-Bis(2-hydroxybenzyl)-1,4-diazacycloheptane (H₂L): 2-Bromomethyl phenylacetate (8.12 g, 35.5 mmol) was added to a solution of DACH (1.54 g, 15.4 mmol) in C₂H₅OH (80 mL) with vigorous stirring at room temperature. Suitable portions of solid KOH were added to the above mixture to ensure that the pH value stayed at 7–8 for ca. 3 days. After filtration of the mixture, the solvent was removed by rotary evaporation. The residue was purified by silica gel column chromatography (CH₂Cl₂/CH₃OH/NH₃·H₂O from 10:10:1 to 5:5:1). The final product was obtained as a white solid in 55% yield (2.65 g, based on DACH). ¹H NMR (CDCl₃): δ = 1.91–1.97 (m, 2 H, CH₂), 2.79–2.85 (m, 8 H, CH₂), 3.80 (s, 4 H, CH₂), 6.75–6.84 (m, 4 H, Ph), 6.94 (d, *J* = 1.5 Hz, 1 H, Ph), 6.96 (d, *J* = 1.5 Hz, 1 H, Ph), 7.14–7.26 (m, 2 H, Ph). IR [KBr pellet (cm⁻¹): 3432 b, 3043 m, 2934 m, 2912 w, 2876 w, 2841 m, 2717 w, 2627 w, 1933 w, 1897 w, 1784 w, 1613 s, 1590 vs, 1479 vs, 1458 vs, 1421s, 1383 w, 1357 s, 1349 s, 1334 m, 1307 w, 1256 vs, 1183 m, 1151 s, 1090 s, 1057 m, 1034 s, 1016 m, 983 s, 936 m, 917 m, 871 m, 850 w, 811 s, 755 vs, 720 m, 625 m, 595 w, 547 m, 459 s. C₁₉H₂₄N₂O₂ (312.41): calcd. C 73.05, H 7.74, N 8.97; found C 73.19, H 7.51, N 8.84.

[Cu₃(μ-L)₂](CH₃OH)₂(ClO₄)₂ (1**):** To a solution of H₂L (63 mg, 0.2 mmol) in CHCl₃ (20 mL) was slowly added a CH₃OH solution (15 mL) of Cu(ClO₄)₂·6H₂O (110 mg, 0.3 mmol) with stirring and a brown powder of complex **1** precipitated gradually. The powder was filtered off, washed with methanol/water and dried under vacuum. Yield: 97 mg (90%). Single crystals of **1** suitable for X-ray analysis were obtained as follows: a solution of Cu(ClO₄)₂·6H₂O in CH₃OH was carefully layered onto a solution of H₂L in CHCl₃ in a 3:2 molar ratio in a straight glass tube and rhombic brown crystals were observed after ca. two weeks. C₄₀H₅₂Cl₂Cu₃N₄O₁₄ (1074.41): calcd. C 44.72, H 4.88, N 5.21; found C 44.61, H 4.74, N 5.17. IR (cm⁻¹): 3446 b, 3061 w, 2940 w, 2905 w, 2860 m, 1598 s, 1574 w, 1482 vs, 1445 s, 1395 m, 1340 w, 1327 w, 1264 s, 1247 vs, 1212 m, 1198 m, 1102 vs, 1061 vs, 970 m, 923 m, 881 m, 864 m, 785 m, 773 s, 763 vs, 761 w, 642 m, 623 s, 577m. Λ_M (CH₃CN): 266 cm² Ω⁻¹ mol⁻¹. λ_{max}/nm (ε/dm³ mol⁻¹ cm⁻¹) (CH₃CN): 558 (220) and 386 (520).

[Ni₃(μ-L)₂(CH₃OH)₂](ClO₄)₂ (2**):** The same synthetic procedure (for both polycrystalline and single-crystal preparation) for **1** was used except that Cu(ClO₄)₂·6H₂O was replaced by Ni(ClO₄)₂·6H₂O. This afforded a red powder in 85% yield (or block-type single crystals). C₄₀H₅₂Cl₂Ni₃N₄O₁₄ (1059.83): calcd. C 45.33, H 4.95, N 5.29; found C 45.61, H 4.58, N 5.04%. IR (cm⁻¹): 3357 b, 3059 w, 3020 w, 2939 w, 2911 w, 2860 m, 1599 s, 1577 m, 1485 vs, 1457 vs, 1398 m, 1342 w, 1325 w, 1261 vs, 1208 m, 1112 vs, 1045 vs, 1027 vs, 972 m, 943 w, 927 m, 883 s, 867 m, 794 s, 767 vs, 734 m, 657 m, 624 s, 605 w, 590 m. Λ_M (H₂O): 182 cm² Ω⁻¹ mol⁻¹. λ_{max}/nm (ε/dm³ mol⁻¹ cm⁻¹) (H₂O): 498 (340), 362 (1150) and 324 (1020).

Caution! Although no problems were encountered in this study, transition metal perchlorate complexes are potentially explosive and should be handled with proper precautions.

Magnetic Studies: The variable-temperature magnetic susceptibilities were measured at the “Servei de Magnetoquímica (Universitat de Barcelona)” on polycrystalline samples (30 mg) with a Quantum Design MPMS SQUID magnetometer operating at a magnetic field of 0.1 T between 2 and 300 K. The diamagnetic corrections were evaluated from Pascal’s constants for all the constituent atoms. Magnetisation measurements were carried out at 2 K in the 0–5 T range. ESR spectra were recorded on powder samples at the X-band frequency with a Bruker 300E automatic spectrometer, varying the temperature between 8 and 298 K.

X-ray Crystallographic Data Collections and Refinements: Single-crystal X-ray diffraction measurements of **1** (brown, 0.30 × 0.25 × 0.20 mm) and **2** (red, 0.30 × 0.25 × 0.20 mm) were carried out with a Bruker Smart 1000 CCD diffractometer equipped with a graphite crystal monochromator situated in the incident beam for data collection at 293(2) K. The lattice parameters were obtained by least-squares refinements of the diffraction data of 781 (for **1**) and 582 (for **2**) reflections, respectively, and data collections were performed with Mo-*K*α radiation (λ = 0.71073 Å) by the ω scan

Table 4. Crystallographic data and structural refinement parameters of complexes **1** and **2**

	1	2
Empirical formula	C ₄₀ H ₅₂ Cl ₂ Cu ₃ N ₄ O ₁₄	C ₄₀ H ₅₂ Cl ₂ Ni ₃ N ₄ O ₁₄
<i>M_r</i>	1074.41	1059.83
Crystal system	monoclinic	triclinic
Space group	<i>P</i> 2 ₁ / <i>n</i>	<i>P</i> 1̄
<i>a</i> (Å)	10.915(4)	9.682(4)
<i>b</i> (Å)	14.208(5)	11.182(4)
<i>c</i> (Å)	14.114(5)	11.278(5)
<i>α</i> (°)	90	76.624(7)
<i>β</i> (°)	98.412(6)	81.561(7)
<i>γ</i> (°)	90	68.404(7)
<i>V</i> (Å ³)	2165.3(13)	1101.9(8)
<i>Z</i>	2	1
<i>D_c</i> [g cm ⁻³]	1.648	1.597
<i>μ</i> [mm ⁻¹]	1.655	1.460
<i>F</i> (000)	1106	550
Total data	10022	4702
Unique data	4392	3850
Data [<i>I</i> > 2σ(<i>I</i>)]	2860	2377
<i>R</i> _{int}	0.0448	0.0322
<i>R</i> ₁ ^[a]	0.0470	0.0447
<i>wR</i> ₂ ^[b]	0.1011	0.0842
GOF ^[c]	1.008	1.011
Residuals [e ⁻ Å ⁻³]	0.575, -0.393	0.340, -0.357

[a] *R*₁ = Σ*F*_o - *F*_c / Σ*F*_o. [b] *wR*₂ = [Σ*w*(*F*_o² - *F*_c²)² / Σ*w*(*F*_o²)²]^{1/2}. [c] GOF = {Σ[*w*(*F*_o² - *F*_c²)²] / (*n* - *p*)^{1/2}.

mode in the range of $2.21 < \theta < 26.39^\circ$ (for **1**) and $2.00 < \theta < 25.00^\circ$ (for **2**). There was no evidence of crystal decay during data collection for both complexes. All the measured independent reflections were used in the structural analyses and semi-empirical absorption corrections were applied using the SADABS program. The program SAINT^[50] was used for integration of the diffraction profiles. Both structures were solved by direct methods using the SHELXS program of the SHELXTL package and refined with SHELXL.^[51] Metal atoms were located from the *E*-maps and other nonhydrogen atoms were located in successive difference Fourier syntheses. The final refinements were performed by full-matrix least-squares methods with anisotropic thermal parameters for all the nonhydrogen atoms on *F*². All hydrogen atoms were first found in difference electron density maps and then placed in the calculated sites and included in the final refinement in the riding model approximation with displacement parameters derived from the parent atoms to which they were bonded. In the refinement of both complexes, a disorder model of the perchlorate anion was used (two constraint components for four oxygen atoms of the perchlorate anion have occupancy factors of 0.5) to make the oxygen atoms exhibit suitable displacement ellipsoids. A summary of the crystallographic data and structure refinements are listed in Table 4. CCDC-232051 (for **1**) and -232052 (for **2**) contains the supplementary crystallographic data for this paper. These data can be obtained free of charge via www.ccdc.cam.ac.uk/cons/retrieving.html (or from the CCDC, 12 Union Road, Cambridge CB2 1EZ, UK; Fax: +44-1223-336-033; E-mail: deposit@ccdc.cam.ac.uk).

Acknowledgments

This work was financially supported by the National Natural Science Foundation of China (No. 20401012) and the Key Project of Tianjin Natural Science Foundation (to M. D.). X. H. B. acknowledges financial support from the Outstanding Youth Foundation of NSFC (No. 20225101) and J. R. from the Spanish Government (Grant BQU2003/00539).

- [1] [1a] D. Gatteschi, *Adv. Mater.* **1994**, *6*, 635–645. [1b] R. E. P. Winpenny, *Comments Inorg. Chem.* **1999**, *20*, 233–262. [1c] S. Leininger, B. Olenyuk, P. J. Stang, *Chem. Rev.* **2000**, *100*, 853–908. [1d] E. I. Solomon, R. K. Szilagyi, S. D. George, L. Basumallick, *Chem. Rev.* **2004**, *104*, 419–458. [1e] D. Gatteschi, R. Sessoli, *Angew. Chem. Int. Ed.* **2003**, *42*, 268–297. [1f] M. A. Halcrow, G. Christou, *Chem. Rev.* **1994**, *94*, 2421–2481.
- [2] For examples, see: [2a] G. A. van Albada, I. Mutikainen, U. Turpeinen, J. Reedijk, *Eur. J. Inorg. Chem.* **1998**, 547–549. [2b] L. Cronin, P. H. Walton, *Inorg. Chim. Acta* **1998**, *269*, 241–245. [2c] T. C. Higgs, K. Spartalian, C. J. O'Connor, B. F. Matzkanke, C. J. Carrano, *Inorg. Chem.* **1998**, *37*, 2263–2272.
- [3] For examples, see: [3a] R. Prins, M. Biagini-Cingi, M. Drillon, R. A. G. de Graaff, J. G. Haasnoot, A. M. Manotti-Lanfredi, P. Rabu, J. Reedijk, F. Uggozzoli, *Inorg. Chim. Acta* **1996**, *248*, 35–44. [3b] P. A. Angaridis, P. Baran, R. Boca, F. Cervantes-Lee, W. Haase, G. Mezei, R. G. Raptis, R. Werner, *Inorg. Chem.* **2002**, *41*, 2219–2228.
- [4] For examples, see: S. Ferrer, J. G. Haasnoot, J. Reedijk, E. Muller, M. B. Cingi, M. Lanfranchi, A. M. M. Lanfredi, J. Ribas, *Inorg. Chem.* **2000**, *39*, 1859–1867.
- [5] For examples, see: [5a] R. L. Beddoes, J. A. Conner, D. Dubowski, A. C. Jones, O. S. Mills, R. Price, *J. Chem. Soc., Dalton Trans.* **1981**, 2119–2126. [5b] L. Gutiérrez, G. Alzuet, J. A. Real, J. Cano, J. Borrás, A. Castiñeiras, *Inorg. Chem.* **2000**, *39*, 3608–3614.
- [6] For examples, see: X. M. Liu, M. P. de Miranda, E. J. L. McInnes, C. A. Kilner, M. A. Halcrow, *Dalton Trans.* **2004**, 59–64.
- [7] For examples, see: J. Ribas, A. Escuer, M. Monfort, R. Vicente, R. Cortes, L. Lezama, T. Rojo, *Coord. Chem. Rev.* **1999**, *195*, 1027–1068.
- [8] [8a] M. Du, X. H. Bu, G. C. Wang, Y. M. Guo, R. H. Zhang, *Inorg. Chim. Acta* **2001**, *320*, 190–197. [8b] M. Du, Y. M. Guo, X. H. Bu, *Inorg. Chim. Acta* **2002**, *335*, 136–140.
- [9] [9a] X. H. Bu, M. Du, L. Zhang, Z. L. Shang, R. H. Zhang, M. Shionoya, *J. Chem. Soc., Dalton Trans.* **2001**, 729–735. [9b] X. H. Bu, M. Du, Z. L. Shang, L. Zhang, Q. H. Zhao, R. H. Zhang, M. Shionoya, *Eur. J. Inorg. Chem.* **2001**, 1551–1558. [9c] M. Du, Z. L. Shang, X. B. Leng, X. H. Bu, *Polyhedron* **2001**, *20*, 3065–3071.
- [10] [10a] X. H. Bu, M. Du, Z. L. Shang, R. H. Zhang, D. Z. Liao, M. Shionoya, T. Clifford, *Inorg. Chem.* **2000**, *39*, 4190–4199. [10b] X. H. Bu, M. Du, L. Zhang, D. Z. Liao, J. K. Tang, R. H. Zhang, M. Shionoya, *J. Chem. Soc., Dalton Trans.* **2001**, 593–598. [10c] M. Du, Y. M. Guo, X. H. Bu, J. Ribas, M. Monfort, *New J. Chem.* **2002**, *26*, 645–650.
- [11] [11a] M. Du, X. H. Bu, Y. M. Guo, L. Zhang, D. Z. Liao, J. Ribas, *Chem. Commun.* **2002**, 1478–1479. [11b] M. Du, X. H. Bu, Y. M. Guo, J. Ribas, C. Diaz, *Chem. Commun.* **2002**, 2550–2551. [11c] M. Du, X. H. Bu, Y. M. Guo, J. Ribas, *Chem. Eur. J.* **2004**, *10*, 1345–1354.
- [12] C. A. Grapperhaus, M. Y. Darensbourg, *Acc. Chem. Res.* **1998**, *31*, 451–459 and references cited therein.
- [13] [13a] D. L. An, Y. M. Guo, M. Du, X. S. Shi, X. H. Bu, *Chin. J. Struct. Chem.* **2004**, *23*, 126–130. [13b] M. Du, Y. M. Guo, S. T. Chen, X. H. Bu, *J. Mol. Struct.* **2002**, *641*, 29. [13c] Y. M. Guo, M. Du, X. H. Bu, *J. Mol. Struct.* **2002**, *610*, 27–31. [13d] M. Du, Y. M. Guo, X. H. Bu, J. Ribas, M. Monfort, *New J. Chem.* **2002**, *26*, 939–945. [13e] Y. M. Guo, Doctor Dissertation, Nankai University.
- [14] [14a] H. Okawa, M. Koikawa, S. Kida, D. Luneau, H. Oshio, *J. Chem. Soc., Dalton Trans.* **1990**, 469–475. [14b] F. Akagi, Y. Nakao, K. Matsumoto, S. Takamizawa, W. Mori, S. Suzuki, *Chem. Lett.* **1997**, 181–182. [14c] W. L. Driessen, L. Chang, C. Finazzo, S. Gorter, D. Rehorst, J. Reedijk, M. Lutz, A. L. Spek, *Inorg. Chim. Acta* **2003**, *350*, 25–31.
- [15] K. Nakamoto, *Infrared and Raman Spectra of Inorganic and Coordination Compounds*, Wiley, New York, **1986**.
- [16] E. V. RybakAkimova, D. H. Busch, P. K. Kahol, N. Pinto, N. W. Alcock, H. J. Clase, *Inorg. Chem.* **1997**, *36*, 510–520.
- [17] G. R. Desiraju, T. Steiner, *The Weak Hydrogen Bond in Structural Chemistry and Biology*, Oxford University Press, **1999**.
- [18] O. Kahn, *Molecular Magnetism*, VCH Publishers, New York, **1993**.
- [19] A. Bencini, D. Gatteschi, *EPR of Exchange Coupled Systems*, Springer-Verlag, Berlin, **1989**.
- [20] L. Banci, A. Bencini, D. Gatteschi, *Inorg. Chem.* **1983**, *22*, 2681–2683.
- [21] R. Veit, J. J. Girerd, O. Kahn, F. Robert, Y. Jeannin, *Inorg. Chem.* **1986**, *25*, 4175–4180.
- [22] R. Costa, A. Garcia, J. Ribas, T. Mallah, Y. Journaux, X. Solans, V. Rodríguez, *Inorg. Chem.* **1993**, *32*, 3733–3742 and references cited therein.
- [23] L. Gutiérrez, G. Alzuet, J. A. Real, J. Cano, J. Borrás, A. Castiñeiras, *Eur. J. Inorg. Chem.* **2002**, 2094–2102.
- [24] V. H. Crawford, H. W. Richardson, J. R. Wason, D. J. Hodgson, W. E. Hatfield, *Inorg. Chem.* **1976**, *15*, 2107–2110.
- [25] [25a] L. Merz, W. Haase, *J. Chem. Soc., Dalton Trans.* **1980**, 875–879. [25b] M. Handa, N. Koga, S. Kida, *Bull. Chem. Soc., Jpn.* **1988**, *61*, 3853–3857.
- [26] K. Nieminen, *Ann. Acad. Sci. Fennicae A II* **1982**, *197*, 1–60.
- [27] L. Walz, H. Paulus, W. Haase, *J. Chem. Soc., Dalton Trans.* **1985**, 913–920.
- [28] A. Bencini, D. Gatteschi, *Inorg. Chim. Acta* **1978**, *31*, 11–18.
- [29] P. J. Hay, J. C. Thibault, R. Hoffman, *J. Am. Chem. Soc.* **1975**, *97*, 4884–4899.
- [30] [30a] O. Kahn, *Inorg. Chim. Acta* **1982**, *62*, 3–14. [30b] J. Comarmond, P. Plumere, J. M. Lehn, Y. Agnus, P. Louis, R. Weiss,

- O. Kahn, I. Morgenstern-Badarau, *J. Am. Chem. Soc.* **1982**, *104*, 6330–6340.
- [31] H. Astheimer, W. Haase, *J. Chem. Phys.* **1986**, *85*, 1427–1432.
- [32] [32a] E. Ruiz, P. Alemany, S. Alvarez, J. Cano, *J. Am. Chem. Soc.* **1997**, *119*, 1297–1303. [32b] E. Ruiz, P. Alemany, S. Alvarez, J. Cano, *Inorg. Chem.* **1997**, *36*, 3683–3688.
- [33] C. Blanchet-Boiteux, J. M. Muesca, *J. Phys. Chem. A* **2000**, *104*, 2091–2097.
- [34] R. J. Butcher, E. Sinn, *Inorg. Chem.* **1976**, *15*, 1604–1608 and references cited therein.
- [35] A. W. Addison, T. N. Rao, J. Reedijk, J. V. Rijn, G. C. Verschoor, *J. Chem. Soc., Dalton Trans.* **1984**, 1349–1356.
- [36] [36a] M. F. Charlot, S. Jeannin, Y. Jeannin, O. Kahn, J. Lucrece-Abaul, J. Martin-Frere, *Inorg. Chem.* **1979**, *18*, 1675–1681. [36b] M. F. Charlot, S. Jeannin, Y. Jeannin, O. Kahn, J. Lucrece-Abaul, J. Martin-Frere, *Inorg. Chem.* **1980**, *19*, 1410–1411.
- [37] [37a] S. Youngme, G. A van Albada, H. Kooijman, O. Roubeau, W. Somjitsripunya, A. L. Spek, C. Pakawatchai, J. Reedijk, *Eur. J. Inorg. Chem.* **2002**, 2367–2374. [37b] I. Castro, M. Julve, G. de Munno, G. Bruno, J. A. Real, F. Lloret, J. Faus, *J. Chem. Soc., Dalton Trans.* **1992**, 1739–1744.
- [38] [38a] S. Youngme, W. Somjitsripunya, K. Chinnakali, S. Chantraproma, H. K. Fun, *Polyhedron* **1999**, *18*, 857–862. [38b] L. P. Wu, M. E. Keniry, B. J. Hathaway, *Acta Crystallogr., Sect. C* **1992**, *48*, 35–40.
- [39] L. K. Thompson, S. K. Mandal, S. S. Tandon, J. N. Bridson, M. K. Park, *Inorg. Chem.* **1996**, *35*, 3117–3125.
- [40] A. M. Greenaway, C. J. O'Connor, J. W. Overman, E. Sinn, *Inorg. Chem.* **1981**, *20*, 1508–1513.
- [41] J. P. Costes, F. Dahan, J. P. Laurent, *Inorg. Chem.* **1985**, *24*, 1018–1022.
- [42] J. M. Seco, U. Amador, M. J. González-Garmendia, *Inorg. Chim. Acta* **2000**, *303*, 256–264.
- [43] G. A. van Albada, I. Mutikainen, I. Riggio, U. Turpeinen, J. Reedijk, *Polyhedron* **2002**, *21*, 141–146.
- [44] H. Saimiya, Y. Sunatsuki, M. Kojima, S. Kashino, T. Kambe, M. Hirotsu, H. Akashi, K. Nakajima, T. Tokii, *Dalton Trans.* **2002**, 3737–3742.
- [45] J. Galy, J. Jaud, O. Kahn, P. Tola, *Inorg. Chim. Acta* **1979**, *36*, 229–236.
- [46] E. Sinn, *Inorg. Chem.* **1976**, *15*, 366–369.
- [47] S. K. Mandal, L. K. Thompson, K. Nag, J. P. Charland, E. J. Gabe, *Inorg. Chem.* **1987**, *26*, 1391–1395.
- [48] J. A. Bertrand, E. Fujita, P. G. Eller, *Inorg. Chem.* **1974**, *13*, 2067–2071.
- [49] R. Range, *Tetrahedron* **1971**, *27*, 1499–1502.
- [50] Bruker AXS, *SAINTE Software Reference Manual*, Madison, WI, **1998**.
- [51] G. M. Sheldrick, *SHELXTL NT Version 5.1. Program for Solution and Refinement of Crystal Structures*, University of Göttingen, Germany, **1997**.

Received July 16, 2004

Early View Article

Published Online November 24, 2004